INORGANIC CHEMISTRY FRONTIERS

CCS 中国化学会 CHINESE CHEMICAL SOCIETY

ROYAL SOCIETY OF CHEMISTRY

Impacts of Ancillary Ligand Coordination Modes on Red-Emitting Cyclometalated Iridium Complexes

Journal:	*Inorganic Chemistry Frontiers*
Manuscript ID	QI-RES-11-2023-002276.R1
Article Type:	Research Article
Date Submitted by the Author:	26-Dec-2023
Complete List of Authors:	Jiang, Chenggang; University of Houston, Chemistry Teets, Thomas; University of Houston, Chemistry

RESEARCH ARTICLE

Impacts of Ancillary Ligand Coordination Modes on Red-Emitting Cyclometalated Iridium Complexes

Received 00th January 20xx,
Accepted 00th January 20xx

DOI: 10.1039/x0xx00000x

Chenggang Jiang and Thomas S. Teets*

Cyclometalated iridium complexes are widely used in optoelectronic technologies, but creating efficient red emitters remains challenging. Prior investigations have demonstrated the efficiency of electron-rich salicylaldimine and 2-picolinamide ligands in promoting red to deep red luminescence. This work introduces a series of ten new red or deep-red emitting heteroleptic bis-cyclometalated iridium(III) complexes supported by eight different ancillary ligands, including some from the salicylaldimine and 2-picolinamide families. Our study reveals that the effectiveness of salicylaldimine ligands at supporting efficient red phosphorescence is dependent on the cyclometalating ligand they are paired with. A more significant finding is that the 2-picolinamide ligands can adopt three different coordination modes. Firstly, the *N*-propyl-substituted 2-picolinamide proligand can bind to the iridium center in its neutral, protonated form through the pyridyl N and amide O atoms, forming five-membered metallacycles. Furthermore, *N*-aryl-substituted ligands can coordinate with the iridium center in either *N*,*N*′ or *N*(pyridyl),*O* modes, yielding two structurally distinct isomers. Notably, the change in coordination mode minimally influences emission wavelength while significantly modulating the photoluminescence quantum yield. This study advances our comprehension of how ligand coordination impacts cyclometalated iridium complexes, offering invaluable insights into the design of high-performance red phosphors for potential optoelectronic applications.

Introduction

Cyclometalated iridium complexes have proven to be highly successful in various applications, such as photovoltaics,[1,2] photocatalysis,[3,4] and bioimaging.[5,6] They are also standout materials for organic light-emitting diodes (OLEDs) due to their unique photophysical properties, including high efficiency, long lifetime, and tunable emission colors.[7–9] Additionally, the good thermal stability of iridium complexes prevents quenching and degradation of emitter materials under high-temperature operation, which is critical for long-term device stability.[10] Currently, there are many available green- or yellow-phosphorescent iridium complexes with near-unity photoluminescence quantum yields.[11–13] These complexes fall into two major structure classes: homoleptic complexes with the general formula $Ir(C^N)_3$ [14,15] and heteroleptic bis-cyclometalated $Ir(C^N)_2(L^X)$ complexes[16,17] (C^N = cyclometalating ligand; L^X = ancillary ligand). The phosphorescence color is generally controlled by the structure of the cyclometalating ligand[18] while the ancillary ligand can impact not only the emission wavelength but also redox properties and excited-state dynamics significantly.[19,20] The ability to fine-tune electronic and optical properties through ligand design enables highly efficient and stable OLEDs with colors spanning the entire visible range.

Despite exceptionally high efficiencies in the green to yellow regions, red-phosphorescent iridium compounds have lower quantum yields, and as a result, the efficiency values of red OLEDs are attenuated.[7,21,22] Low-energy excited states tend to exhibit slow radiative rates, given the cubic dependence of the radiative rate constant (k_r) on the transition energy.[23] Moreover, nonradiative decay rates (k_{nr}) are inversely related to HOMO-LUMO gaps via the energy-gap law,[24] mainly due to the strong overlap of vibrational energy levels between the ground and excited states. Our group has used the ancillary ligand structure to maximize the photoluminescence quantum yields in the red region,[25–29] and a few other groups have also made significant contributions with related approaches.[30–33] Our strategy has centered on electron-rich, π-donating ancillary ligands, which destabilize the HOMO, increase the metal d-orbital participation and spin-orbit coupling in the excited state, and thus augment k_r values.[28,34]

Some of our most recent work showed that substituted salicylaldimine and 2-picolinamide derivatives are particularly effective at supporting efficient phosphorescence in the red region and beyond.[35] Despite many works that have been done to evaluate the impact of different ancillary ligands on photoluminescence, few studies reveal the influence of varying coordination modes of the same ligand on luminescence properties.[36,37] From the standpoint of fundamental coordination chemistry, it is essential to understand the varied

University of Houston, Department of Chemistry, 3585 Cullen Blvd., Room 112, Houston, TX USA 77204-5003
*Email: tteets@uh.edu
† Electronic Supplementary Information (ESI) available: X-ray crystallography summary table, NMR spectra, IR spectra, additional cyclic voltammetry data, and excitation spectra (PDF). See DOI: 10.1039/x0xx00000x

ways certain ancillary ligands can bind to the metal, and how these different coordination modes affect the photophysical properties of iridium complexes will establish fundamental structure-property relationships that may lead to advances in the performance of red phosphors.

With these insights in mind, we report ten new complexes in this work. One subset of these compounds involves pairing the ancillary ligands we previously reported with different cyclometalating ligands, making four new complexes to evaluate the combined effects the cyclometalating ligands and ancillary ligands have on the photoluminescence properties. During this investigation, we noticed that 2-picolinamide analogues sometimes produce multiple products, and with further inquiry discovered that 2-picolinamide ancillary ligands can exhibit three distinct coordination modes. The structures of those distinct binding modes, the reaction conditions that favor one over the other, and the thermal interconversion between them are all described. Finally, three new ancillary ligands were introduced, allowing evaluation of the effects of donor atom identity and substituents on the electronic structure. The photophysical properties of all ten complexes, via UV–vis absorption and photoluminescence spectroscopy, are thoroughly outlined along with their electrochemical characteristics measured by cyclic voltammetry (CV). This study shows that salicylaldimine and picolinamide ancillary ligands are efficient in supporting the red-emitting iridium complexes provided the emissive excited state maintains substantial metal-to-ligand charge transfer (MLCT) character. Another important photophysical consequence is that the different coordination modes of the 2-picolinamide ancillary ligand do not significantly perturb the emission wavelength but largely alter the photoluminescence quantum yields. On the whole, this work further elaborates the utility of salicylaldimine, 2-picolinamide, and related ancillary ligands in the design of red-phosphorescent compounds, supporting a diverse range of structure types with appealing photophysical metrics.

Results and Discussion

Synthesis and structural characterization

In our previous study salicylaldimines were one particularly effective class of ancillary ligands for red-phosphorescent compounds,[35] and here we include an expanded set of such complexes with different cyclometalating ligands or different substitution patterns on the salicylaldimine ligand. Scheme 1 outlines the synthetic method for four salicylaldimine complexes following the previously reported procedure. Three cyclometalating ligands (C^N = 2-(2-pyridyl)benzothiophene (btp), 1-phenylisoquinoline (piq), and 6-phenylphenanthridine (pphen)) were chosen to make the target complexes with emission in the red to deep red region. The *N*-propyl (**L^1**) and *N*-tolyl (**L^2**) salicylaldimine variants were previously used by our group in combination with piq and a cyano-substituted piq variant.[35] Our previous work also showed that 4-trifluoromethylphenyl was a particularly effective substituent in 2-picolinamide ancillary ligands (see below), so in this study we

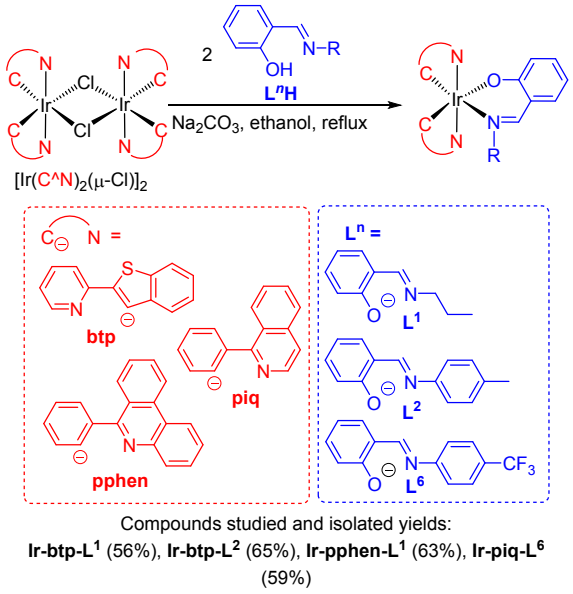

Scheme 1 Synthesis of salicylaldimine compounds.

also introduced a salicylaldimine variant **L^6** with the same *N*-substituent, pairing it with the piq cyclometalating ligand. All four new compounds were characterized by a combination of NMR spectroscopy (Fig. S1–S7) and high-resolution mass spectrometry. The complexes **Ir-btp-L^1**, **Ir-btp-L^2**, and **Ir-piq-L^6** were also characterized by single-crystal X-ray diffraction. Their molecular structures are shown in Fig. 1, with detailed crystallographic data reported in Tables S1. As we have observed,[35] the ancillary ligand C–O bond distances are intermediate between typical single and double-bond lengths, consistent with π-delocalization into the ancillary ligand core. The O–Ir–N bite angles for these six-member chelate

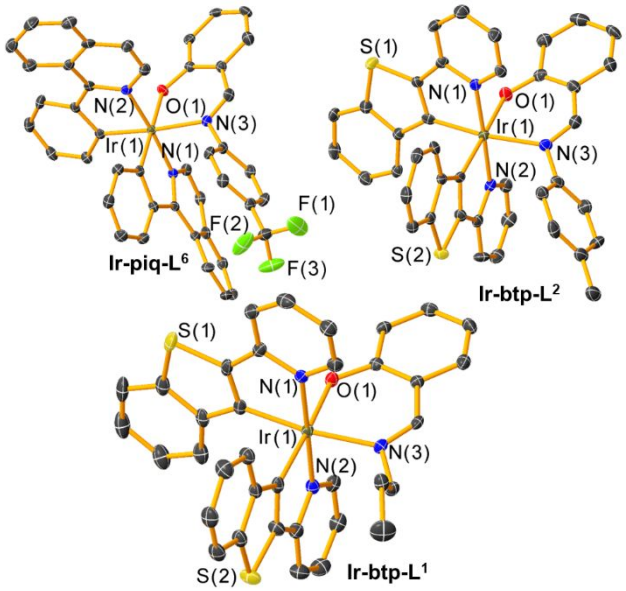

Fig. 1 Molecular structures of **Ir-btp-L^1**, **Ir-btp-L^2**, and **Ir-piq-L^6**, determined by single-crystal X-ray diffraction. Thermal ellipsoids are shown at the 50% probability level. Hydrogen atoms and solvent molecules were omitted for clarity.

salicylaldimine complexes are similar, spanning a narrow range of 87.23(12)° – 88.90(7)°.

While further investigating and expanding the library of compounds containing 2-picolinamide ancillary ligands, we found that different coordination modes of this ligand class can be favored depending on the substitution pattern and reaction conditions, as summarized in Scheme 2. The identity and purity of four new compounds are validated by NMR spectroscopy (Fig. S8–15), high-resolution mass spectrometry, and IR spectroscopy (Fig. S20–S28). To denote the three distinct binding modes, **L^N** indicates the typical *N*,*N*′ coordination involving pyridyl and amide nitrogen atoms with the ligand in its deprotonated, monoanionic state. **L^N-B** indicates an isomeric form where the ligand is still monoanionic but binds instead in an *N*(pyridyl),*O* fashion. Finally, **L^{N}H-B** is used when the ligand likewise binds through the pyridyl nitrogen and amide oxygen, but is in its neutral, protonated form, thus giving a cationic complex.

The complex **Ir-piq-L^{3}H-B**, in which the 2-picolinamide binds in its neutral, protonated state through pyridine and oxygen, was first observed as a minor product when reproducing the previously reported **Ir-piq-L^3** complex.[35] After optimizing reaction conditions, the complex **Ir-piq-L^{3}H-B** can be synthesized in good yield by treating $[Ir(piq)_2(\mu\text{-}Cl)]_2$ dimer with the ancillary ligand **L^{3}H** at room temperature in THF, in the absence of base. The ^{1}H NMR shows one additional downfield proton resonance at 11.80 ppm for the amide N–H (Fig. S8), which is not present when the 2-picolinamide binds in a deprotonated, monoanionic form. High-resolution mass spectrometry confirms the ligand protonation state in **Ir-piq-L^{3}H-B**. The X-ray crystal structure of **Ir-piq-L^{3}H-B** cannot be well-refined due to poor crystal quality, but nonetheless the connectivity of **Ir-piq-L^{3}H-B** was confirmed with the low-resolution structure displayed in Fig. S29. The complex is clearly cationic with a chloride counteranion, with the 2-picolinamide binding to iridium through the pyridine N atom and the amide O atom.

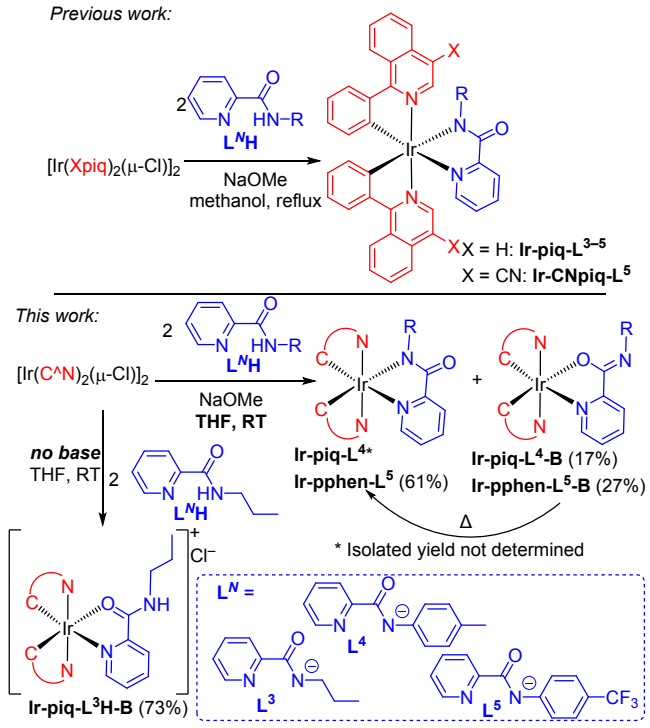

Scheme 2. Synthesis of 2-picolinamide compounds with new coordination modes.

Changing the reaction conditions also leads to a secondary product when combining aryl-substituted 2-picolinamides with $[Ir(C^N)_2(\mu\text{-}Cl)]_2$ dimers. Previously we obtained **Ir-piq-L$^{3–5}$** and **Ir-CNpiq-L^5** (Scheme 2) by combining the chloride-bridged dimers and the 2-picolinamide proligand in basic methanol under reflux.[35] Altering the C^N ligand to pphen, we successfully synthesized the targeted complex **Ir-pphen-L^5** in good yield using modified conditions where the solvent was changed to THF and the reaction was carried out at room temperature. However, under these conditions a secondary species formed, which was separated chromatographically and identified as **Ir-pphen-L^5-B**, featuring the alternative *N*(pyridyl),*O* binding mode. The analogous complex **Ir-piq-L^4-B** also forms under the same reaction conditions, along with the previously synthesized **Ir-piq-L^4**. ^{1}H NMR spectra of these minor products (Fig. S10 and S14) indicate they have the same number of protons as the target complexes, and HRMS-ESI gives the same molecular weight for both the major and minor products. Taken together, these analyses suggest the two products from each reaction are isomers. Single-crystal X-ray diffraction of **Ir-pphen-L^5-B** unambiguously confirmed the structure, which is shown in Fig. 2. Refinement data for this structure are summarized in Table S2. This complex includes a previously unobserved 2-picolinamide chelating mode involving the pyridyl nitrogen and the amide oxygen. The ancillary ligand C–O bond distance is 1.297(7) Å, similar to what we observed in other O-donor ligands.[35,38] The C–C distance from the 2-position of the pyridine ring to the amide C=O carbon (1.512(8) Å) is consistent with a C–C single bond, indicating no π-delocalization. The amide C–N distance is 1.289(7) Å, significantly shorter than the typical secondary amide C–N bond and suggestive of a dominant imine resonance with a C=N double bond. The absence of a counter anion in the crystal structure confirms that **Ir-pphen-L^5-B** is a neutral complex with the 2-picolinamide ancillary ligand in a deprotonated, monoanionic form. The O–Ir–N bite angle in this

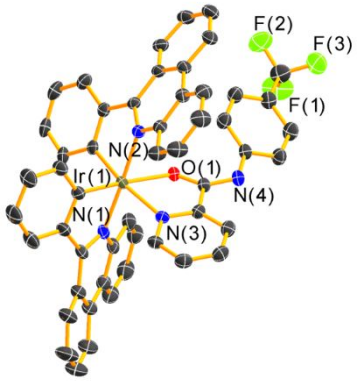

Fig. 2 Molecular structure of **Ir-pphen-L^5-B**, determined by single-crystal X-ray diffraction. Thermal ellipsoids are shown at the 50% probability level. Hydrogen atoms bonded to carbon and solvent molecules were omitted for clarity.

five-member chelate 2-picolinamide complex is 75.71(16)°, very similar to the bite angle in the *N*,*N*′ chelating 2-picolinamide complexes **Ir-piq-L^4** and **Ir-piq-L^5**.[35]

FT–IR can also distinguish the different binding modes in the 2-picolinamide complexes. The C=O stretching frequency shifts to a lower frequency in the case of **Ir-piq-L^{3}H-B** compared to the free ligand **L^{3}H**, and we observe a further decrease in the complex **Ir-piq-L^3**. On the other hand, the complex **Ir-piq-L^4** has a higher C=O stretching frequency than its isomer **Ir-piq-L^4-B**, with the same trend observed in the **Ir-pphen-L^5** and **Ir-pphen-L^5-B** pair. Notably, complexes that adopt the same coordination mode have similar C=O stretching frequencies; for example, $\tilde{\nu}_{C=O}$ in **Ir-piq-L^4-B** and **Ir-pphen-L^5-B** are identical, and both have a sizable redshift compared to the isomers **Ir-piq-L^4** and **Ir-pphen-L^5**. Another interesting finding is that **Ir-piq-L^4-B** and **Ir-pphen-L^5-B** can be thermally transformed to **Ir-piq-L^4** and **Ir-pphen-L^5** under mild heating, as shown in Fig. S30–S31. After refluxing for seven days in THF-d_8, almost all of the *N*(pyridine),*O*-coordinated complexes irreversibly convert to *N*,*N*′-coordinated compounds. Therefore, we assign the *N*(pyridine),*O*-coordinated complexes (**Ir-piq-L^4-B** and **Ir-pphen-L^5-B**) as kinetic products, and the *N*,*N*′-coordinated compounds (**Ir-piq-L^4** and **Ir-pphen-L^5**) are the thermodynamically favored products.

In this work we also investigated two new structurally-related *N*,*N*′-chelating ancillary ligands, paired with the cyclometalating ligand piq. The syntheses of **Ir-piq-L^7**, isolated as its PF_6^- salt, and neutral complex **Ir-piq-L^8**, are outlined in Scheme 3. Both of these products were characterized by NMR spectroscopy and HRMS-ESI. The compound **Ir-piq-L^7** was prepared by treating 1 equivalent of the $[Ir(piq)_2(\mu\text{-}Cl)]_2$ dimer with 2.5 equiv of **L^7** in the presence of 2.1 equiv of silver hexafluorophosphate ($AgPF_6$). The synthesis of **Ir-piq-L^8** started by treating the **L^{8}H** proligand with *n*-butyllithium in THF at −35 °C. The resultant deprotonated ligand was then combined with the chloro-bridged cyclometalated iridium dimer, slowly warmed to room temperature, and stirred overnight. Both compounds were purified by recrystallization and isolated in moderate to good yields. The complex **Ir-piq-L^8** was also characterized by single-crystal X-ray diffraction, and its structure is depicted in Fig. 3, with detailed crystallographic data reported in Table S3. The N–Ir–N bite angle in this six-member chelate complex is 86.79(11) °, aligned with what we observed in other six-member chelate complexes.[38,39]

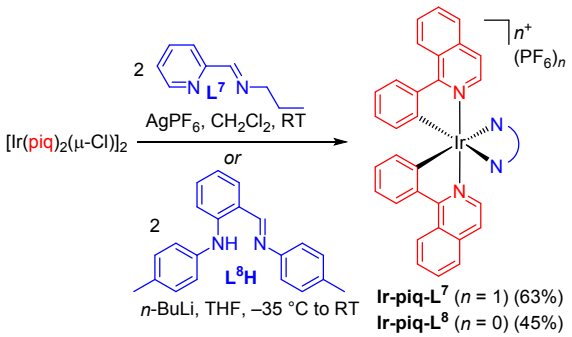

Scheme 3 Synthesis of complexes **piq-L^7[PF$_6$]** and **piq-L^8**.

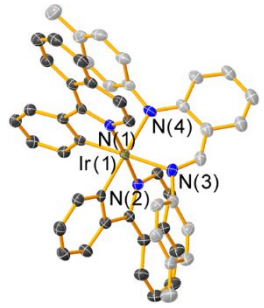

Fig. 3 Molecular structure of **Ir-piq-L^8**, determined by single-crystal X-ray diffraction. Thermal ellipsoids are shown at the 50% probability level. Hydrogen atoms bonded to carbon were omitted for clarity. The carbon atoms of the ancillary ligand are shown in gray to provide additional contrast.

Electrochemistry

The electrochemical properties of the complexes were studied by cyclic voltammetry in anaerobic THF solutions. The overlaid voltammograms are shown in Fig. 4, with the redox potentials reported relative to the ferrocene couple (Fc^+/Fc) and summarized in Table 1. Complexes **Ir-btp-L^1** and **Ir-btp-L^2** have similar quasi–reversible reduction potentials; however, replacing the *N*-propyl group (**Ir-btp-L^1**) with *N*-tolyl (**Ir-btp-L^2**) causes a negative shift in oxidation potential. The complex **Ir-pphen-L^1** has a much more positive reduction potential than the btp analog with the same ancillary ligand, suggesting substantial stabilization of the LUMO energy. However, the oxidation potential shows less dependence on the cyclometalating ligand, indicating the cyclometalating ligands only have minor contributions to the HOMO. Complex **Ir-piq-L^6** shows a reversible first reduction peak at −2.27 V, which becomes irreversible when sweeping to even more negative potentials (Fig. S32). With the second reduction wave observed at −2.49 V, the reduction profile of **Ir-piq-L^6** is very similar to what we observed in other compounds with the same cyclometalating ligand, which can be assigned as the

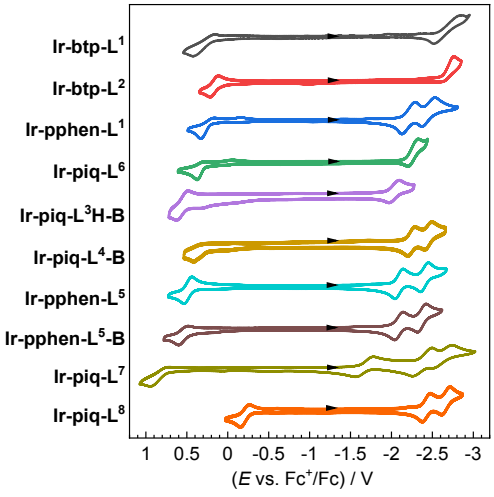

Fig. 4 Cyclic voltammograms of all complexes recorded in THF with 0.1 M $TBAPF_6$ electrolyte. Currents are normalized to bring all the traces into the same scale, and the arrows indicate the scan direction.

Table 1 Summary of redox potentials for all complexes, measured by cyclic voltammetry.

	E^{ox} / V	E^{red} / V
Ir-btp-L^1	0.29[a]	−2.68
Ir-btp-L^2	0.17	−2.69
Ir-pphen-L^1	0.25[a]	−2.21, −2.45
Ir-piq-L^6	0.32[a]	−2.27, −2.49, −2.77
Ir-piq-L^{3}H-B	0.56	−2.03, −2.46, −2.65
Ir-piq-L^4-B	0.37	−2.24, −2.45
Ir-pphen-L^5	0.48	−2.10, −2.41
Ir-pphen-L^5-B	0.54	−2.09, −2.37
Ir-piq-L^7	0.83[a]	−1.67, −2.38, 2.63
Ir-piq-L^8	−0.21	−2.42, −2.66

[a] Irreversible wave; the half-peak potential[40] is reported.

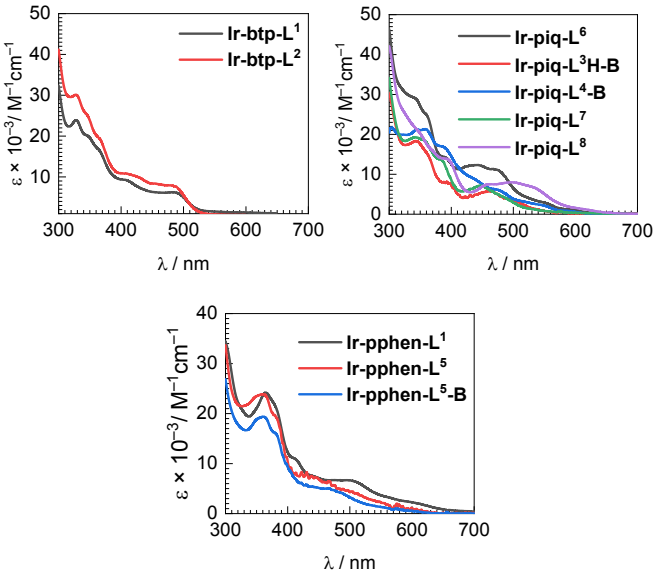

Fig. 5 Overlaid UV–vis absorption spectra of iridium complexes, recorded in toluene at room temperature and organized by cyclometalating ligand.

subsequent reduction of each C^N ligand. Compared to the previously reported **Ir-piq-L^4**, changing the ancillary ligand donor atom from *O* to *N* in **Ir-piq-L^8** results in a significant cathodic shift in oxidation and reduction potential, as seen in other red-emitting complexes. Cationic complexes **Ir-piq-L^{3}H-B** and **Ir-piq-L^7** exhibit three reduction waves, with similar potentials for the second and third reductions that likely indicate subsequent population of a π* orbital on each C^N ligand. The first reduction peak in these two cationic complexes depends strongly on the ancillary ligand and occurs at a much more positive potential than typically observed when C^N = piq, suggesting that the LUMO in these compounds is mainly centered on the neutral ancillary ligand. In complex **Ir-piq-L^4-B**, the reduction potentials are shifted anodically to a small extent compared to **Ir-piq-L^4**, and the same trend can be observed in the pair of **Ir-pphen-L^5** and **Ir-pphen-L^5-B**. For these aryl-substituted 2-picolinamide complexes that exist in two isomeric forms, the oxidation and reduction potentials and the associated HOMO and LUMO energy levels are only slightly dependent on the ancillary ligand coordination mode.

Photophysics

The UV–vis absorption spectra were recorded in toluene solution at room temperature for all complexes. The overlaid absorption spectra grouped by different C^N ligands are displayed in Fig. 5. In all cases, the intense absorption bands in the UV region (λ < 350 nm) are assigned to the spin-allowed ligand-centered π→π* transitions. The less intense, overlapping absorption bands extending beyond 500 nm for btp and beyond 600 nm for piq complexes can be assigned as both singlet and triplet metal-to-ligand charge transfer (^{1}MLCT/^{3}MLCT) transitions, consistent with other well-characterized bis-cyclometalated iridium complexes.[27,38,41] These bands tail to longer wavelengths in the pphen complexes, which align with their smaller HOMO–LUMO gaps.

Fig. 6 collects the room-temperature photoluminescence spectra of the iridium complexes, whereas Table 2 summarizes the data. The excitation spectra are shown in the ESI† (Fig. S34–S43) and overlay very well with the UV–vis absorption spectra, indicating no impurities are interfering with the observed emission. Consistent with our previous report on C^N = piq analogues, the complex **Ir-btp-L^1** with the *N*-propyl substituted salicylaldimine ancillary ligand has a much higher solution quantum yield than *N*-tolyl substituted analogue **Ir-btp-L^2**, primarily because of a more than 7× higher k_{nr} value in the latter, and the ancillary ligand substituent does not perturb the emission peak wavelengths. However, the photoluminescence quantum yields of both btp complexes are moderate in solution (Φ_{PL} = 0.34 and 0.07 for **Ir-btp-L^1** and **Ir-btp-L^2**, respectively), and their k_r values in both solution and PMMA film, spanning in the range of 0.74–1.2 × 10^5 s^{-1}, are not significantly different than many other C^N = btp complexes with different ancillary ligands.[38] This suggests that salicylaldimine ancillary ligands aren't particularly effective at promoting red phosphorescence with high quantum yields and fast radiative rates when btp is the cyclometalating ligand. The sharp vibronic structure in the PL of these compounds (first two panels of Fig. 6) indicates there is significant btp ^{3}(π→π*) character in the emissive T_1 state, which we have shown in previous studies generally leads to electron-rich ancillary ligands *not* being effective at promoting high Φ_{PL} values.[28,38,42]

In contrast, the broad PL of the remaining compounds with poorly resolved vibronic structure is suggestive of significant ^{3}MLCT character in the T_1 state, which results in the PL maxima and k_r values being strongly responsive to the ancillary ligand.[28,34] As expected, complex **Ir-pphen-L^1** exhibits luminescence with a maximum well beyond 650 nm (Fig. 6, third row), with Φ_{PL} = 0.30 in toluene solution and 0.41 in PMMA, the differences arising primarily from a decrease in k_{nr} value in the polymer film. Although its quantum yield is not as high as

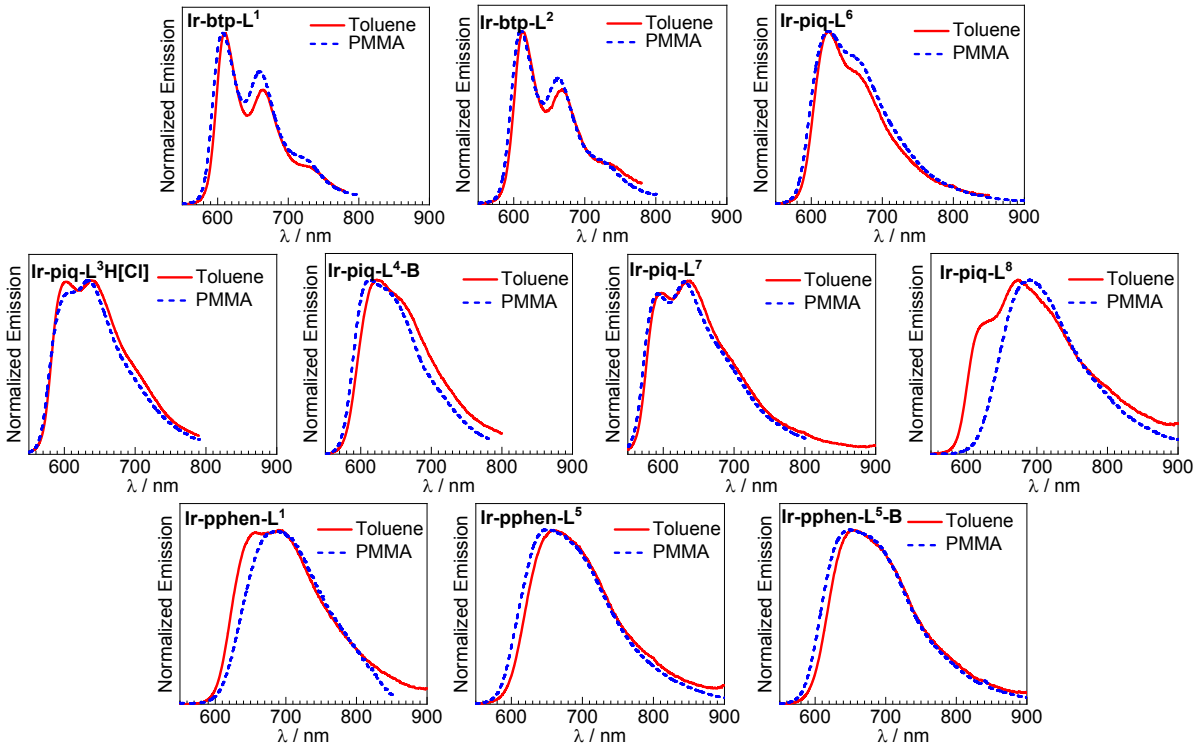

Fig. 6 Overlaid photoluminescence spectra of all complexes, recorded at room temperature. The emission spectra were recorded in both toluene (red solid line) and as a 2 wt% transparent PMMA film (blue dashed line). Samples were excited at 420 nm.

Table 2. Summary of photoluminescence data for all complexes.

	Toluene				2 wt% in PMMA				
	λ / nm	Φ_{PL}	τ / μs	($k_r \times 10^{-5}$ /s^{-1}) / ($k_{nr} \times 10^{-5}$ /s^{-1})	λ / nm	Φ_{PL}	τ / μs	($k_r \times 10^{-5}$ /s^{-1}) / ($k_{nr} \times 10^{-5}$ /s^{-1})	(CIEx, CIEy)
Ir-btp-L^1	611, 665, 740(sh)	0.34	2.9	1.2/1.3	607, 658, 731(sh)	0.62	5.4	1.1/0.70	(0.66, 0.34)
Ir-btp-L^2	612, 669, 739(sh)	0.07	0.95	0.74/9.8	631, 667(sh)	0.56	5.6	1.0/0.79	(0.67, 0.33)
Ir-pphen-L^1	696, 755(sh)	0.30	0.72	4.2/9.7	686	0.41	1.0	4.1/5.9	(0.70, 0.30)
Ir-piq-L^6	625, 669(sh)	0.08	0.15	5.3/61	624, 670(sh)	0.66	1.2	5.5/2.8	(0.67, 0.33)
Ir-piq-L^{3}H-B	603, 638, 706(sh)	0.84	1.2	7.0/1.3	601(sh), 631	0.94	1.4	6.7/0.43	(0.64, 0.36)
Ir-piq-L^4-B	625, 664(sh)	0.02	0.56	0.36/18	611, 651(sh)	0.40	1.3	3.1/4.6	(0.65, 0.35)
Ir-pphen-L^5	659	0.30	1.4	2.1/5.0	652	0.69	1.6	4.3/1.9	(0.69, 0.31)
Ir-pphen-L^5-B	653	0.21	0.70	3.0/11	649	0.39	1.3	3.0/4.7	(0.68, 0.32)
Ir-piq-L^7	596, 637, 705(sh)	0.13	1.2	1.1/7.3	592(sh), 630	0.32	1.7	1.9/4.0	(0.61, 0.39)
Ir-piq-L^8	620(sh), 673	0.002	1.3	0.012/5.9	690	0.17	1.4	1.2/5.9	(0.71, 0.29)

previously reported CNpiq analogues which luminesce in a similar spectral region,[35] complex **Ir-pphen-L^1** does have a very fast radiative decay rate (k_r = 4.2 × 10^5 s^{-1} in solution), rivaling or exceeding other previously reported deep-red phosphorescent complexes with the same cyclometalating ligand.[25,26] Another structural effect we investigated is replacing the *N*-tolyl group in **L^2** with 4-trifluoromethylphenyl in **L^6**, hypothesizing that the CF_3 group can suppress k_{nr} as we observed in complexes of the 2-picolinamide analogue **L^5**, including previously reported[35] **Ir-piq-L^5** and **Ir-CNpiq-L^5**, and, to a lesser extent, **Ir-pphen-L^5** (see Scheme 2 for structures). The photoluminescence properties completely refute this hypothesis. The emission profile remains unperturbed in **Ir-piq-L^6** (Fig. 6) and the k_r has the same magnitude, but this trifluoromethylated complex exhibits a more than threefold increase in the nonradiative rate constant in solution compared to tolyl-substituted analog. These values lead to a moderate Φ_{PL} in solution (0.08), which increases considerably in PMMA film (Φ_{PL} = 0.66) due to a suppression of k_{nr}. Substituting the donor atom in *N*-tolyl salicylaldimine to produce **L^8**, i.e., replacing the oxygen with a second *N*-tolyl, results in significantly redshifted emission to the deep-red region, corresponding to the smaller electrochemical HOMO–LUMO gap. The photoluminescence quantum yields of **Ir-piq-L^8** are low both in both solution and PMMA film, with the inherently low k_r value primarily responsible.

In the 2-picolinamide complexes, the different observed coordination modes can subtly affect the emission wavelength but profoundly impact the excited state dynamics. The complex **Ir-piq-L^{3}H-B** (Fig. 6, middle row) shows exceptionally strong red

luminescence (Φ_{PL} = 0.84) in fluid toluene solution with an emission maximum of 638 nm and has a near-unity quantum yield when immobilized in PMMA film, with Φ_{PL} = 0.94. The λ_{0-0} wavelength in **Ir-piq-L^{3}H-B** shifts to shorter wavelength by ca. 24 nm (635 cm^{-1}) relative to **Ir-piq-L^3**,[35] which can be tentatively explained by the neutral, protonated ancillary ligand being less electron-rich. The compound **Ir-piq-L^7** was introduced as a point of comparison to **Ir-piq-L^{3}H-B**. Both complexes are cationic, whereas **Ir-piq-L^7** replaces the amide oxygen donor atom in **Ir-piq-L^{3}H-B** with an imine nitrogen atom. The amide complex **Ir-piq-L^{3}H-B** has more than 6× higher Φ_{PL} than the imine complex **Ir-piq-L^7**, even though the emission wavelengths are very similar. Given the very low-energy LUMO indicated by the cyclic voltammogram of **Ir-piq-L^7** (Fig. 4), it seems likely there is a deactivating, nonemissive state in this complex that centers on the diimine ancillary ligand. *N*(pyridyl)-*O*-bound 2-picolinamide complexes **Ir-piq-L^4-B** and **Ir-pphen-L^5-B** have almost identical emission profiles with their structural isomers **Ir-piq-L^4** and **Ir-pphen-L^5**, but significant lower Φ_{PL} values. These decreases in Φ_{PL} are primarily due to much larger k_{nr} values and have subtle contributions from declines in k_r. Our tentative explanation is that this alternative binding mode places the *N*-aryl substituent distal to the bis-cyclometalated iridium fragment, allowing it to freely rotate and contribute to nonradiative decay pathways. In contrast, in the "normal" *N*,*N*′ binding mode this *N*-aryl ring closely approaches an adjacent C^N ligand, likely restricting its rotation.

Although the main purpose of this study was to investigate the effects of different ancillary ligand structures and binding modes on photoluminescence properties, it is worthwhile to briefly contextualize the quantum yield values against related compounds in the literature. The red-phosphorescent iridium compounds used in some of the most efficient literature-reported OLEDs all have photoluminescence quantum yields near 0.5.[18,22,43] A recent advance from Kim *et al.* has produced a red cyclometalated iridium OLED dopant with near-unity quantum yield,[33] and some of our best-performing examples with electron-rich ancillary ligands exhibit Φ_{PL} > 0.8 in solution and/or PMMA film.[28,35] Most of the compounds in this study fall short of these standout examples, excepting **Ir-piq-L^{3}H-B**, which has near-unity photoluminescence quantum yields in solution and polymer film, albeit with luminescence that is not as deep red as some of the previously cited examples. The three new deep-red-emitting compounds with C^N = pphen have quantum yields that rival some of our best-performing examples with PL maxima beyond 650 nm,[25,26,34,42] although they are not clearly superior. In short, most of the compounds in this work have very good photoluminescence quantum yields for the red region of the spectrum, although there are certainly other compounds in the literature with superior metrics.

Experimental

General procedures for the synthesis of compounds described here and their photophysical characterization are given below. The ESI† includes full synthetic details and physical characterization data.

General synthetic procedure. For most compounds, the chloro-bridged cyclometalated iridium dimer [Ir(C^N)$_2$(μ-Cl)]$_2$ was treated with base and the ancillary proligand **L^{N}H**. For the cationic complexes **Ir-piq-L^{3}H-B** and **Ir-piq-L^7** the base was omitted and in the latter case $AgPF_6$ was included to extract chloride. The reaction mixture was stirred at room temperature or refluxed for 12–24 hours, and the final product was purified by column chromatography and/or recrystallization. Characterization by ^{1}H and ^{13}C{^{1}H} NMR and high-resolution mass spectrometry confirmed the identity and purity of the product.

Photophysical measurements. UV–vis absorption spectra were measured in toluene solutions in 1 cm quartz cuvettes sealed with a screw cap and septum, using an Agilent Cary 8454 UV–vis spectrophotometer. Steady-state emission spectra were measured using a Horiba FluoroMax-4 spectrofluorometer with appropriate long-pass filters to exclude stray excitation light from detection. To exclude air, samples for emission spectra were prepared in a nitrogen-filled glovebox using dry, deoxygenated solvents, and thin-film PMMA samples were kept under nitrogen until immediately before measurement. Photoluminescence quantum yields of solution samples were determined relative to a standard of tetraphenylporphyrin (TPP) in toluene, which has a reported fluorescence quantum yield (Φ_F) of 0.11.[44] The absolute quantum yields of complexes doped into poly(methyl methacrylate) (PMMA) thin films were recorded using a Spectralon-coated integrating sphere integrated with a Horiba FluoroMax-4 spectrofluorometer.

Conclusions

This work presents a study on the effects of ancillary ligand structure parameters and coordination modes on the excited states of red-emitting cyclometalated iridium complexes. Here, we report ten novel cyclometalated iridium red emitters, including eight different ancillary ligands, which can form six different coordination cores. We had previously introduced salicylaldimine and 2-picolinamide ligands as particularly effective at promoting red phosphorescence. These salicylaldimine ligands are less effective when the cyclometalating ligand is btp, which produces red phosphorescence with more C^N-ligand-centered character. Substituting the hydroxy group in salicylaldimine derivatives with an aryl amine suppresses the radiative rate constant (k_r) and significantly redshifts the emission wavelength. A significant new insight from this work is that the 2-picolinamide ligands can adopt three different coordination modes. First, the *N*-propyl substituted 2-picolinamide proligand (**L^{3}H**) can bind to the iridium center in its neutral form via an *N*(pyridyl),*O* mode, forming five-member metallacycles. Moreover, the *N*-aryl substituted ligands can coordinate to the iridium center in an analogous *N*,*O* mode but in a monoanionic deprotonated state, in addition to the usual *N*,*N*′ mode we observed before. Complexes with the monoanionic *N*,*O* mode, which can thermally transform to the more stable *N*,*N*′-coordinated complexes, have much lower Φ_{PL} than their structural isomers. In total, this work gave new insights into the coordination

chemistry of these ancillary ligand classes and produced a series of red to deep-red phosphors, some with exceptional photoluminescence quantum yields in solution and/or polymer film. This work reveals critical fundamental insights into controlling and optimizing phosphorescence by controlling the ligand coordination mode and donor atom identity.

Author Contributions

Chenggang Jiang: Conceptualization, formal analysis, investigation, visualization, writing – original draft, writing – review & editing.

Thomas S. Teets: Conceptualization, funding acquisition, project administration, supervision, visualization, writing – review & editing.

Conflicts of interest

There are no conflicts to declare.

Acknowledgements

We acknowledge the Welch Foundation (Grant E-1887) and the National Science Foundation (Grant CHE-1846831) for funding this work.

Notes and references

1 T. Yang, B. Wang, Y. He, A. Zhou, Z. Yao, G. Xing and Y. Tao, Triplet Homoleptic Iridium(III) Complex as a Potential Donor Material for Organic Solar Cells, *Inorg. Chem.*, 2023, **62**, 5920–5930.

2 M. Lee, T.-H. Kwon and T. Kim, Synergetic Effect of the Iridium Complex for Morphology Optimization in Efficient and Thermally Stable Polymer Solar Cells, *J. Phys. Chem. C*, 2023, **127**, 9522–9528.

3 L. Xu, P. Deng, W. Song, M. Liu, M. Wang, Y. Yu and F. Wang, An AIE-Active Cyclometalated Iridium(III) Photosensitizer for Selective Discrimination, Imaging, and Synergistic Elimination of Gram-Positive Bacteria, *ACS Mater. Lett.*, 2023, **5**, 162–171.

4 W. Lin, Y. Liu, J. Wang, Z. Zhao, K. Lu, H. Meng, R. Luoliu, X. He, J. Shen, Z.-W. Mao and W. Xia, Engineered Bacteria Labeled with Iridium(III) Photosensitizers for Enhanced Photodynamic Immunotherapy of Solid Tumors, *Angew. Chem.*, **n/a**, e202310158.

5 Z. Feng, J. Xian, F. Chen, Y. Wang, Y. Tian, J. Sun and X. Tian, Intermolecular interactions enhanced second harmony generation of iridium complex for bio-labeling, *Chem. Eng. J.*, 2023, **458**, 141503.

6 Y. Ma, D. Zhang, W. Lv, Q. Zhao and W.-Y. Wong, Water-soluble iridium(III) complexes as multicolor probes for one-photon, two-photon and fluorescence lifetime imaging, *J. Organomet. Chem.*, 2023, **992**, 122697.

7 G. Hong, X. Gan, C. Leonhardt, Z. Zhang, J. Seibert, J. M. Busch and S. Bräse, A Brief History of OLEDs—Emitter Development and Industry Milestones, *Adv. Mater.*, 2021, **33**, 2005630.

8 A. R. G. Smith, P. L. Burn and B. J. Powell, Spin–Orbit Coupling in Phosphorescent Iridium(III) Complexes, *ChemPhysChem*, 2011, **12**, 2429–2438.

9 M. A. Baldo, D. F. O'Brien, Y. You, A. Shoustikov, S. Sibley, M. E. Thompson and S. R. Forrest, Highly efficient phosphorescent emission from organic electroluminescent devices, *Nature*, 1998, **395**, 151–154.

10 I. N. Mills, J. A. Porras and S. Bernhard, Judicious Design of Cationic, Cyclometalated Ir(III) Complexes for Photochemical Energy Conversion and Optoelectronics, *Acc. Chem. Res.*, 2018, **51**, 352–364.

11 T. Sajoto, P. I. Djurovich, A. B. Tamayo, J. Oxgaard, W. A. I. Goddard and M. E. Thompson, Temperature Dependence of Blue Phosphorescent Cyclometalated Ir(III) Complexes, *J. Am. Chem. Soc.*, 2009, **131**, 9813–9822.

12 T.-Y. Li, J. Wu, Z.-G. Wu, Y.-X. Zheng, J.-L. Zuo and Y. Pan, Rational design of phosphorescent iridium(III) complexes for emission color tunability and their applications in OLEDs, *Coord. Chem. Rev.*, 2018, **374**, 55–92.

13 P. Tao, W.-L. Li, J. Zhang, S. Guo, Q. Zhao, H. Wang, B. Wei, S.-J. Liu, X.-H. Zhou, Q. Yu, B.-S. Xu and W. Huang, Facile Synthesis of Highly Efficient Lepidine-Based Phosphorescent Iridium(III) Complexes for Yellow and White Organic Light-Emitting Diodes, *Adv. Funct. Mater.*, 2016, **26**, 881–894.

14 X. Li, J. Zhang, Z. Zhao, L. Wang, H. Yang, Q. Chang, N. Jiang, Z. Liu, Z. Bian, W. Liu, Z. Lu and C. Huang, Deep Blue Phosphorescent Organic Light-Emitting Diodes with CIEy Value of 0.11 and External Quantum Efficiency up to 22.5%, *Adv. Mater.*, 2018, **30**, 1705005.

15 Z. Chen, L. Wang, S. Su, X. Zheng, N. Zhu, C.-L. Ho, S. Chen and W.-Y. Wong, Cyclometalated Iridium(III) Carbene Phosphors for Highly Efficient Blue Organic Light-Emitting Diodes, *ACS Appl. Mater. Interfaces*, 2017, **9**, 40497–40502.

16 X. Liang, F. Zhang, Z.-P. Yan, Z.-G. Wu, Y. Zheng, G. Cheng, Y. Wang, J.-L. Zuo, Y. Pan and C.-M. Che, Fast Synthesis of Iridium(III) Complexes Incorporating a Bis(diphenylphorothioyl)amide Ligand for Efficient Pure Green OLEDs, *ACS Appl. Mater. Interfaces*, 2019, **11**, 7184–7191.

17 C. Jiang, L. M. Cañada, N. B. Nguyen, M. D. S. Halamicek, S. H. Nguyen and T. S. Teets, Substituent-Dependent Azide Addition to Isocyanides Generates Strongly Luminescent Iridium Complexes, *J. Am. Chem. Soc.*, 2023, **145**, 1227–1235.

18 S. Lamansky, P. Djurovich, D. Murphy, F. Abdel-Razzaq, H.-E. Lee, C. Adachi, P. E. Burrows, S. R. Forrest and M. E. Thompson, Highly Phosphorescent Bis-Cyclometalated Iridium Complexes: Synthesis, Photophysical Characterization, and Use in Organic Light Emitting Diodes, *J. Am. Chem. Soc.*, 2001, **123**, 4304–4312.

19 J. Li, P. I. Djurovich, B. D. Alleyne, M. Yousufuddin, N. N. Ho, J. C. Thomas, J. C. Peters, R. Bau and M. E. Thompson, Synthetic Control of Excited-State Properties in Cyclometalated Ir(III) Complexes Using Ancillary Ligands, *Inorg. Chem.*, 2005, **44**, 1713–1727.

20 Y. You and S. Y. Park, Inter-Ligand Energy Transfer and Related Emission Change in the Cyclometalated Heteroleptic Iridium Complex: Facile and Efficient Color Tuning over the Whole Visible Range by the Ancillary Ligand Structure, *J. Am. Chem. Soc.*, 2005, **127**, 12438–12439.

21 J. C. Deaton, R. H. Young, J. R. Lenhard, M. Rajeswaran and S. Huo, Photophysical Properties of the Series fac- and mer-(1-Phenylisoquinolinato-NΛC2')x(2-phenylpyridinato-NΛC2')3−xIridium(III) (x = 1−3), *Inorg. Chem.*, 2010, **49**, 9151–9161.

22 A. Tsuboyama, H. Iwawaki, M. Furugori, T. Mukaide, J. Kamatani, S. Igawa, T. Moriyama, S. Miura, T. Takiguchi, S. Okada, M. Hoshino and K. Ueno, Homoleptic Cyclometalated Iridium

Complexes with Highly Efficient Red Phosphorescence and Application to Organic Light-Emitting Diode, *J. Am. Chem. Soc.*, 2003, **125**, 12971–12979.
23 H. Yersin, *Highly efficient OLEDs with phosphorescent materials*, Wiley-VCH, Weinheim, 2008.
24 R. Englman and J. Jortner, The energy gap law for radiationless transitions in large molecules, *Mol. Phys.*, 1970, **18**, 145–164.
25 S. Yoon and T. S. Teets, Enhanced deep red to near-infrared (DR-NIR) phosphorescence in cyclometalated iridium(III) complexes, *Inorg. Chem. Front.*, 2022, **9**, 6544–6553.
26 S. Yoon, T. G. Gray and T. S. Teets, Enhanced Deep-Red Phosphorescence in Cyclometalated Iridium Complexes with Quinoline-Based Ancillary Ligands, *Inorg. Chem.*, 2023, **62**, 7898–7905.
27 P. Lai, S. Yoon, Y. Wu and T. S. Teets, Effects of Ancillary Ligands on Deep Red to Near-Infrared Cyclometalated Iridium Complexes, *ACS Org. Inorg. Au*, 2022, **2**, 236–244.
28 P.-N. Lai, C. H. Brysacz, M. K. Alam, N. A. Ayoub, T. G. Gray, J. Bao and T. S. Teets, Highly Efficient Red-Emitting Bis-Cyclometalated Iridium Complexes, *J. Am. Chem. Soc.*, 2018, **140**, 10198–10207.
29 Y. K. Radwan, A. Maity and T. S. Teets, Manipulating the Excited States of Cyclometalated Iridium Complexes with β-Ketoiminate and β-Diketiminate Ligands, *Inorg. Chem.*, 2015, **54**, 7122–7131.
30 Ł. Skórka, M. Filapek, L. Zur, J. G. Małecki, W. Pisarski, M. Olejnik, W. Danikiewicz and S. Krompiec, Highly Phosphorescent Cyclometalated Iridium(III) Complexes for Optoelectronic Applications: Fine Tuning of the Emission Wavelength through Ancillary Ligands, *J. Phys. Chem. C*, 2016, **120**, 7284–7294.
31 P. Tao, Y. Zhang, J. Wang, L. Wei, H. Li, X. Li, Q. Zhao, X. Zhang, S. Liu, H. Wang and W. Huang, Highly efficient blue phosphorescent iridium(III) complexes with various ancillary ligands for partially solution-processed organic light-emitting diodes, *J. Mater. Chem. C*, 2017, **5**, 9306–9314.
32 F. Monti, F. Kessler, M. Delgado, J. Frey, F. Bazzanini, G. Accorsi, N. Armaroli, H. J. Bolink, E. Ortí, R. Scopelliti, Md. K. Nazeeruddin and E. Baranoff, Charged Bis-Cyclometalated Iridium(III) Complexes with Carbene-Based Ancillary Ligands, *Inorg. Chem.*, 2013, **52**, 10292–10305.
33 S. Kim, J. Kim, J. Choi, M. Sim, Y. Koishikawa, Y. Cho, S. Kim, S. Kwak, A. Jeon, O. Kwon, D. Lee, J. Y. Lee and B. Choi, Rational Ligand Design of Heteroleptic Iridium (III) Complexes toward Nearly Perfect Horizontal Dipole Orientation for Highly Efficient Red-Emitting Phosphorescent Organic Light-Emitting Diodes, *Adv. Funct. Mater.*, 2023, **33**, 2214233.
34 S. Yoon and T. S. Teets, Red to near-infrared phosphorescent Ir(III) complexes with electron-rich chelating ligands, *Chem. Commun.*, 2021, **57**, 1975–1988.
35 C. Jiang, S. Yoon, Y. H. Nguyen and T. S. Teets, Modular Imine Chelates with Variable Anionic Donors Promote Red Phosphorescence in Cyclometalated Iridium Complexes, *Inorg. Chem.*, 2023, **62**, 11278–11286.
36 S. A. Moore, D. L. Davies, M. M. Karim, J. K. Nagle, M. O. Wolf and B. O. Patrick, Photophysical behaviour of cyclometalated iridium(III) complexes with phosphino(terthiophene) ligands, *Dalton Trans.*, 2013, **42**, 12354–12363.
37 A. J. Wilkinson, A. E. Goeta, C. E. Foster and J. A. G. Williams, Synthesis and Luminescence of a Charge-Neutral, Cyclometalated Iridium(III) Complex Containing NΛCΛN- and CΛNΛC-Coordinating Terdentate Ligands, *Inorg. Chem.*, 2004, **43**, 6513–6515.
38 P. Lai and T. S. Teets, Ancillary Ligand Effects on Red-Emitting Cyclometalated Iridium Complexes, *Chem. – Eur. J.*, 2019, **25**, 6026–6037.
39 G. Mu, C. Jiang and T. S. Teets, Dinuclear Complexes of Flexidentate Pyridine-Substituted Formazanate Ligands, *Chem. – Eur. J.*, 2020, **26**, 11877–11886.
40 E. M. Espinoza, J. A. Clark, J. Soliman, J. B. Derr, M. Morales and V. I. Vullev, Practical Aspects of Cyclic Voltammetry: How to Estimate Reduction Potentials When Irreversibility Prevails, *J. Electrochem. Soc.*, 2019, **166**, H3175–H3187.
41 P.-N. Lai, S. Yoon and T. S. Teets, Efficient near-infrared luminescence from bis-cyclometalated iridium(III) complexes with rigid quinoline-derived ancillary ligands, *Chem. Commun.*, 2020, **56**, 8754–8757.
42 E. Kabir, Y. Wu, S. Sittel, B.-L. Nguyen and T. S. Teets, Improved deep-red phosphorescence in cyclometalated iridium complexes via ancillary ligand modification, *Inorg. Chem. Front.*, 2020, **7**, 1362–1373.
43 C.-H. Fan, P. Sun, T.-H. Su and C.-H. Cheng, Host and Dopant Materials for Idealized Deep-Red Organic Electrophosphorescence Devices, *Adv. Mater.*, 2011, **23**, 2981–2985.
44 P. G. Seybold and M. Gouterman, Porphyrins: XIII: Fluorescence spectra and quantum yields, *J. Mol. Spectrosc.*, 1969, **31**, 1–13.